

TSC1 involvement in bladder cancer: diverse effects and therapeutic implications

Yanan Guo,¹ Yvonne Chekaluk,¹ Jianming Zhang,² Jinyan Du,³ Nathanael S Gray,² Chin-Lee Wu⁴ and David J Kwiatkowski^{1*}

¹ Division of Translational Medicine, Department of Medicine, Brigham and Women's Hospital and Harvard Medical School, Boston, MA, USA

² Dana Farber Cancer Institute, Harvard Medical School, Boston, MA, USA

³ Broad Institute of Harvard University and Massachusetts Institute of Technology, Cambridge, MA, USA

⁴ Departments of Pathology and Urology, Massachusetts General Hospital, Boston, MA, USA

*Correspondence to: DJ Kwiatkowski, Division of Translational Medicine, Department of Medicine, Brigham and Women's Hospital and Harvard Medical School, Boston, MA 02115, USA. E-mail: dk@rics.bwh.harvard.edu

Abstract

TSC1 is often mutated in bladder cancer. However the importance of this event in disease pathogenesis and its implications for therapy are uncertain. We used genomic sequencing to examine the involvement of *TSC1* in bladder cancer, and signalling pathway analysis and small-molecule screening to identify targeted therapeutic strategies in *TSC1* mutant bladder cancer cell lines. *TSC1* loss of heterozygosity was seen in 54% of bladder cancers. Two (4.9%) of these 41 bladder cancers had *TSC1* mutations by exon-based sequencing. Analysis of 27 bladder cancer cell lines demonstrated inactivating *TSC1* mutations in three: RT-4, HCV29, 97-1. Interestingly, only RT-4 showed classic feedback inhibition of AKT, and was highly sensitive to treatment with mTOR inhibitors rapamycin and Torin1. 97-1 cells showed constitutive EGFR activation, and were highly sensitive to combined treatment with the mTOR inhibitor Torin1 and EGFR inhibitors Lapatinib or Afatinib. A *BRAF* missense mutation G469V was found in HCV29 cells, and AKT activation was dependent on *BRAF*, but independent of ERK. A kinase inhibitor screen of HCV29 cells showed strong growth inhibition by the Hsp90 inhibitor NVP-AUY922, and we then found synergistic inhibitory effects of NVP-AUY922 combined with either Torin1 or rapamycin on cell survival for both HCV29 and 97-1 cells. In aggregate, these findings indicate that there are highly variable mutation profiles and signalling pathway activation in *TSC1*-mutant bladder cancer. Furthermore, combined Hsp90/mTOR inhibition is a promising therapeutic approach for *TSC1* mutant bladder cancer.

Copyright © 2013 Pathological Society of Great Britain and Ireland. Published by John Wiley & Sons, Ltd.

Keywords: TSC1; TSC2; bladder cancer; kinase inhibitor; Torin1

Received 24 December 2012; Revised 23 January 2013; Accepted 2 February 2013

No conflicts of interest were declared.

Introduction

Bladder cancer is the fourth most common cancer overall and the second most common urological malignancy in the USA [1]. Urothelial (transitional cell) carcinoma is the most common histological subtype in the USA [2]. Bladder cancer is thought to be caused by multiple environmental and genetic factors and is associated with advanced age [3]. Early studies identified frequent loss of heterozygosity (LOH) for all of chromosome 9 in many bladder cancers, likely targeting *CDKN2A* on 9p [4]. The other *CDKN2A* allele is commonly disrupted by focal deletion events, point mutation or DNA methylation [5]. However, several studies have shown that 10–15% of bladder cancers have inactivating point mutations of *TSC1* on 9q34, which, in combination with large-scale deletion or chromosome 9 loss, led to complete loss of functional *TSC1* [6–8]. In addition, loss of a single *TSC1* allele (haplo-insufficiency)

may provide a growth advantage to bladder epithelial cells, contributing to bladder cancer development [9]. Furthermore, a recent report identified a *TSC1* mutation in a bladder cancer patient with metastatic disease who had a sustained complete response to treatment with the mTOR inhibitor everolimus [10].

Both *TSC1* and *TSC2* cause the autosomal dominant genetic disorder tuberous sclerosis complex (TSC), in which individuals develop a variety of benign but often progressive neoplasms [11]. The protein products of *TSC1* and *TSC2* form the TSC1–TSC2 protein complex, which plays a critical role in growth control as a primary regulator of the mammalian target of rapamycin (mTOR) pathway [12–14]. TSC1–TSC2 acts as a GTPase activating protein (GAP) toward RHEB, while RHEB–GTP activates mTOR complex 1 (mTORC1). The mTOR serine–threonine kinase exists in cells in two complexes, mTORC1 and mTORC2. mTORC1 phosphorylates a number of

downstream proteins, including the S6 kinases and 4EBP1 [15,16]. Constitutive activation of mTORC1 occurs in cells lacking either TSC1 or TSC2, leading to unregulated ribosome and protein biogenesis, cell size increase and preparation for cell division and growth.

Here we sought to examine the role of *TSC1* mutation in bladder cancer, with a focus on identification of therapeutic strategies. After confirming mutations in *TSC1* in a fraction of human bladder cancers, we studied three *TSC1*-null bladder cancer cell lines to examine signalling pathways and growth sensitivities in the setting of TSC1–TSC2 complex loss. We found diversity among the cell lines studied, with responses by some but not all to specific targeted therapies. Moreover, combined Hsp90/mTOR inhibition appeared promising for treatment of *TSC1* mutant bladder cancer.

Materials and methods

Human samples

Bladder cancer and normal bladder samples were identified from the pathological archives of the Massachusetts General Hospital. These materials were discarded samples from patients undergoing surgical procedures. Consent was obtained from each patient and the study was approved by the Partners Human Research Committee. Bladder cancer staging and grade was determined according to WHO standards [2]. Pathological samples embedded in paraffin were reviewed by CW to determine the percentage tumour purity in each. Frozen samples were prepared from adjacent tumour samples and were expected to have roughly the same purity.

Reagents

LY294002 was purchased from Biomol Research Laboratories (Plymouth Meeting, PA, USA). Torin1, Afatinib and PLX-4032 were generously provided by Nathanael Gray, Pasi Jänne and Krishna Vasudevan, respectively (all at Dana Farber Cancer Institute, Boston, MA, USA). Lapatinib and rapamycin were obtained from LC laboratories (Woburn, MA, USA). U0126 was purchased from Sigma-Aldrich (St. Louis, MO, USA). The cell culture medium Dulbecco's modified Eagle's medium (DMEM) was from Cellgro (Manassas, VA, USA) and supplements were from Invitrogen (Carlsbad, CA, USA).

Cell culture, viral expression and viability assays

Twenty-four bladder cancer cell lines (MGH-U1, MGH-U3, MGH-U4, MGH-U5, UMUC1, UMUC3, UMUC6, UMUC7, UMUC10, UMUC11, UMUC15, UMUC17, RT-4, T-24, HT1376, SCaBER, 253J, HT1197, 5637, J82, 647V, BL13, BL17 and BL128)

were available from the Translational Urology Research Laboratory at Massachusetts General Hospital (MA, USA). Two bladder cell lines (HCV29, 97–1) were kindly provided by Margaret A Knowles (St James's University Hospital, UK) and 639V was obtained from the Leibniz Institute DSMZ – German Collection of Microorganisms and Cell Cultures (Germany). All cell lines were maintained in DMEM supplemented with 10% fetal bovine serum (FBS) and 1% penicillin–streptomycin–amphotericin B (PSA) in an incubator at 37 °C in 5% CO₂. For serum starvation, cells were cultured in the absence of serum for 24 h. Serum was then added back at 10% final concentration for 30 min for stimulation. To replace TSC1 expression in cell lines lacking a functional gene, HEK293T cells were transfected with a set of viral packaging vectors and pLXIN empty vector or pLXIN-TSC1 lentivirus vector (obtained from Hongbing Zhang, Beijing, China). Supernatant containing virus was collected and filtered through a 0.45 µm filter. *TSC1*-null cells were infected with the supernatant containing virus overnight and then selected with and maintained in hygromycin. For cell viability assays, cells were plated in sterile 96-well plates and cultured overnight. Compounds were then added in serial dilutions. Cellular viability was determined after 48 h, using Vybrant® MTT Cell Proliferation Assay Kit (Invitrogen). Plates were measured on a THERMOmax microplate reader (Molecular Devices).

Immunoblotting and immunoprecipitation

Cells were harvested in lysis buffer consisting of 50 mM Tris–HCl, pH 7.5, 150 mM NaCl, 1% Triton X-100, 1 mM EDTA, 1 mM EGTA and a cocktail of protease inhibitors (Sigma-Aldrich). Cell lysates were clarified by centrifugation for 5 min and the protein concentration of supernatants determined using a modified Bradford assay (Bio-Rad, Hercules, CA, USA). For immunoblotting, 20 µg protein was loaded in each lane and separated by SDS–PAGE on 4–12% gradient gels (Invitrogen), transferred to PVDF membranes and detected with the following primary antibodies: TSC1 (no. 4906), pAKT(S473) (no. 4060), AKT (no. 9272), pS6(S240/244) (no. 2215), S6 (no. 2217), PTEN (no. 9559), LKB1 (no. 3050), Raptor (no. 2280), Rictor (no. 2114), pS6K(T389) (no. 9205), S6K (no. 9202), pERK (Y202/Y204) (no. 9101), ERK (no. 9102), pEGFR(Y1086) (no. 2220), EGFR (no. 2232), cleaved caspase 3 (no. 9661), IRS1 (no. 2382), p4EBP1(S65) (no. 9451), 4EBP1 (no. 9452), and BRAF (no. 9434) (all from Cell Signalling Technology); TSC2 (sc-893; Santa Cruz Biotechnology), goat anti-mouse and anti-rabbit secondary antibodies (Santa Cruz Biotechnology) conjugated to horseradish peroxidase were used at a 1:3000 dilution and immunoreactive bands detected by chemiluminescence (SuperSignal, Pierce, Rockford, IL, USA) and film (Denville Scientific, South Plainfield, NJ, USA).

For immunoprecipitation, 500 µg clarified cell lysate were pre-absorbed with 50 µl protein A/G Sepharose (GE Healthcare, Piscataway, NJ, USA) for 1 h at 4 °C and incubated overnight at 4 °C with 1 µg antibody. Immune complexes were precipitated with 50 µl protein A/G Sepharose for 1 h and then washed three times with lysis buffer. Immunoprecipitated proteins were eluted in Laemmli sample buffer, separated by SDS-PAGE and immunoblotted as outlined above.

Kinome tyrosine kinase phosphorylation profiling

Luminex immunosandwich assays were performed as previously described [23], with the following modifications. Antibodies were conjugated to Luminex MagPlex microspheres (Luminex). Assays were carried out in 384-well ThermoMatrix square-bottomed plates (Thermo) in conjunction with a 96-well (CyBio) and a 384-well (BioMek) liquid handler. Data were acquired with a FlexMap 3D instrument (Luminex), according to the manufacturer's instructions, and normalized by subtracting sample and antibody backgrounds. A normalized value > 10 was considered positive. Marker selection and heatmap generation were performed with GENE-E software (<http://www.broadinstitute.org/cancer/software/GENE-E/>).

DNA analysis methods

DNA from fresh-frozen bladder cancer samples and cDNA from cell lines were sequenced by Sanger methodology for all coding exons (3–23) of *TSC1*, using primers described previously [17]. Sequencing for *FGFR3* mutations was performed for exons 7, 10 and 15, using primers shown in Table S1 (see Supplementary material). OncoMap mutation analysis was performed in a multiplexed mass spectrometry assay, interrogating 983 unique mutations in 115 genes [26], at the Center for Cancer Genome Discovery at the Dana Farber Cancer Institute.

A molecular inversion probe (MIP) assay was used to determine the signal intensity for each allele of 330 000 SNPs (Affymetrix, Santa Clara, CA, USA) [38] on bladder cancer DNA samples extracted from formalin-fixed paraffin-embedded (FFPE) samples, using the Qiagen DNA Purification kit. A full description of this methodology and global analysis of results has been submitted elsewhere for publication [39]. FFPE-extracted DNA samples were sent to Affymetrix and processed at their facility in Santa Clara, CA. Briefly, the raw MIP intensity data provided by Affymetrix were analysed using Nexus Copy Number v. 6.0 (BioDiscovery, El Segundo, CA, USA), normalized using the SNP-FASST2 segmentation algorithm. Normalized probe intensity and allele ratio data were visualized in Nexus v. 6.0. Probes (20–30 each) from the region of *TSC1* on chromosome 9 and from the region of *TSC2* on chromosome 16 were visually assessed in Nexus to determine the copy number and allele ratios in these regions.

Kinase inhibitor library screen

A small compound, kinase inhibitor-focused library (LINCS) was used to screen cell lines for sensitivity to kinase inhibitors. The LINCS library consists of 197 commercially available kinase inhibitors, as well as in-house developed pharmacophore-diverse ATP competitive kinase inhibitors targeting either active or inactive kinase conformations (see Supplementary material, Table S2). Compounds in the LINCS library were each chosen to be relatively potent and selective toward a narrow range of kinase targets. Kinase inhibitor screening was performed at the concentration of 660 nM, with or without added rapamycin (25 nM) or Torin1 (50 nM) in a 2 day cellular proliferation assay, in which cells were plated and drug added simultaneously on day 0. Drug effects on growth were determined using CellTiter-Glo (Promega, WI, USA). IC₅₀ determinations were performed by similar means, using Cell-Titer-Glo in 96-well plates. However, cells were plated on day 0, drug was added on day 1 and cell growth was determined on day 3 in this assay format. Compounds were serially diluted three-fold from 10 µM to 1.5 nM. The IC₅₀ was determined using XLfit4.0 software (ID Business Solutions, Burlington, MA, USA).

Statistical analysis

Quantitative data are reported as the mean ± standard error of the mean (SEM) from at least three independent experiments. The means for various treatment groups were compared using analysis of variance (ANOVA) and Dunnett's *post hoc* test.

Results

Analysis of *TSC1* and *TSC2* in bladder cancer samples

To examine the frequency of *TSC1* and *TSC2* involvement in human bladder cancer, we used two approaches. First, a MIP assay (see Methods for details) was used to examine genomic copy number and LOH across the *TSC1* and *TSC2* regions on FFPE samples. Twenty-two (54%) of 41 bladder cancer samples showed LOH for *TSC1* and 13 (32%) of 41 showed LOH for *TSC2* (see Supplementary material, Table S3). LOH of *TSC1* was seen in all stages of bladder cancer, suggesting that it was not associated with any particular stage or grade ($p > 0.76$, ANOVA), although the sample number is not large. Second, we performed exon-based Sanger sequencing of the coding region of *TSC1* on fresh-frozen samples from these same cancers, and identified *TSC1*-inactivating mutations in two (5%) of the 41 samples (see Supplementary material, Table S3, Figure S1A, B). These were a single base deletion mutation and a nonsense mutation, and are clearly inactivating.

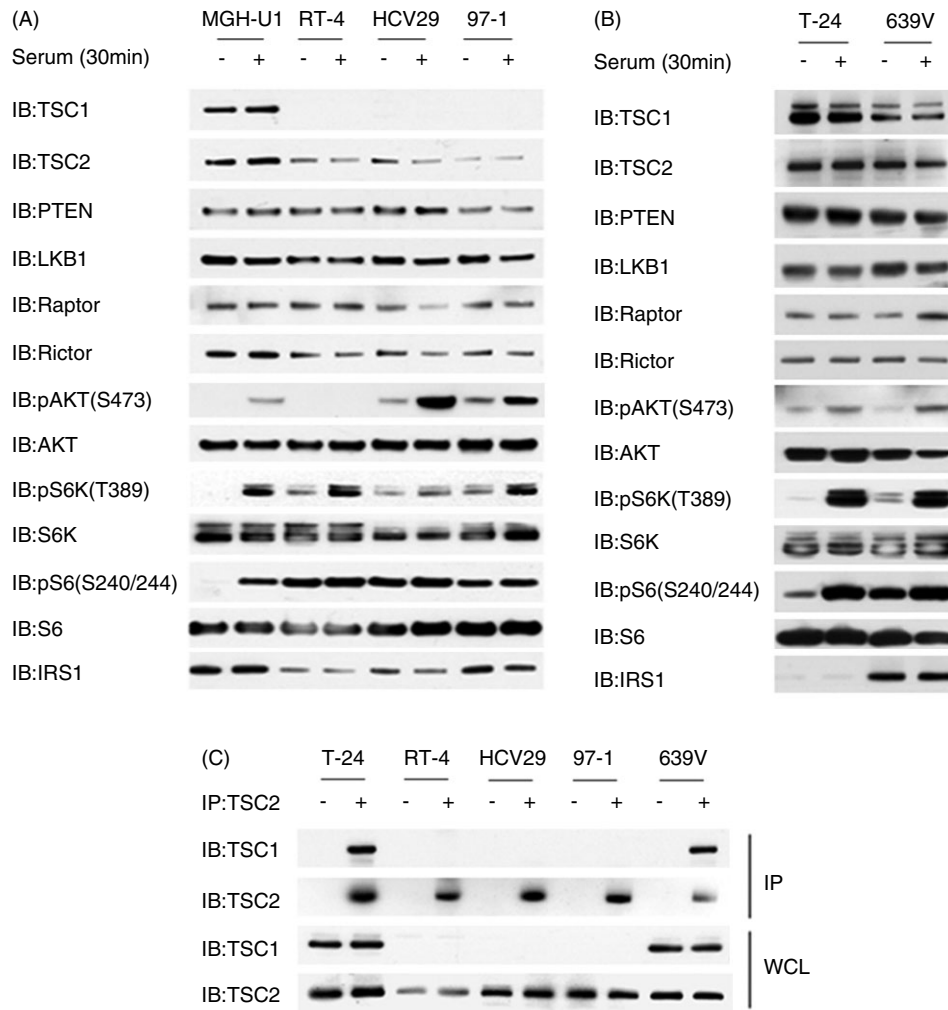


Figure 1. Identification and characterization of *TSC1*-null bladder cancer cell lines. (A, B) Immunoblots of bladder cancer cell lines after 24 h of serum starvation (–) or 30 min after serum add-back following serum starvation (+), for multiple components of the AKT–mTOR signalling pathways. The RT-4, HCV29, 97–1 and 639V cell lines have *TSC1* mutations; the first three do not express *TSC1*; MGH-U1 and T-24 are controls. (C) Immunoprecipitation of the *TSC1*–*TSC2* protein complex using a *TSC2* antibody. Both whole-cell lysates (WCL) and protein immunoprecipitates (IP) were analysed by immunoblotting.

Analysis of *TSC1* and *TSC2* in bladder cancer cell lines

To explore further the involvement of *TSC1* and *TSC2* in bladder cancer, we examined *TSC1* expression in a collection of 27 bladder cancer cell lines by immunoblotting. This set included four cell lines previously reported to have a mutation in *TSC1* [6]. Three of these lines, RT-4, HCV29 and 97–1, showed complete absence of *TSC1* expression (Figure 1A; see also Supplementary material, Table S4). These three lines also showed homozygous inactivating *TSC1* mutations by sequence analysis (see Supplementary material, Figure S1) [17], consistent with complete loss of *TSC1* expression. The fourth cell line, 639V, had two *TSC1* missense mutations, as reported [17], but expressed *TSC1* protein (Figure 1B), which formed a complex with *TSC2* by co-immunoprecipitation (Figure 1C), suggesting that the *TSC1* protein expressed might be functional. In contrast, this same assay confirmed a complete lack of expression of *TSC1* in RT-4, HCV29

and 97–1 (Figure 1C). Therefore, we focused our studies on RT-4, HCV29 and 97–1.

Immunoblot analysis showed that RT-4, HCV29 and 97–1 all showed reduced *TSC2* expression (Figure 1A), consistent with previous studies indicating that *TSC1* plays an important function in stabilizing *TSC2* [18]. Levels of PTEN, LKB1, Raptor, AKT, S6K and S6 were similar among these cell lines and a control bladder cancer cell line, MGH-U1 (Figure 1A). RT-4 showed absence of AKT activation, as assessed by phospho-AKT-S473 (pAKT-S473) levels, in both serum-deprived and serum add-back conditions. This suggests the presence of an active feedback suppression loop in the AKT–mTOR pathway due to constitutive mTORC1 activation, as seen in many other cell lines lacking *TSC1* or *TSC2* [19,20]. However, neither HCV29 nor 97–1 showed this phenomenon, instead showing some level of pAKT-S473 during serum deprivation and robust AKT activation in response to serum add-back (Figure 1A). Note that Rictor expression, an essential

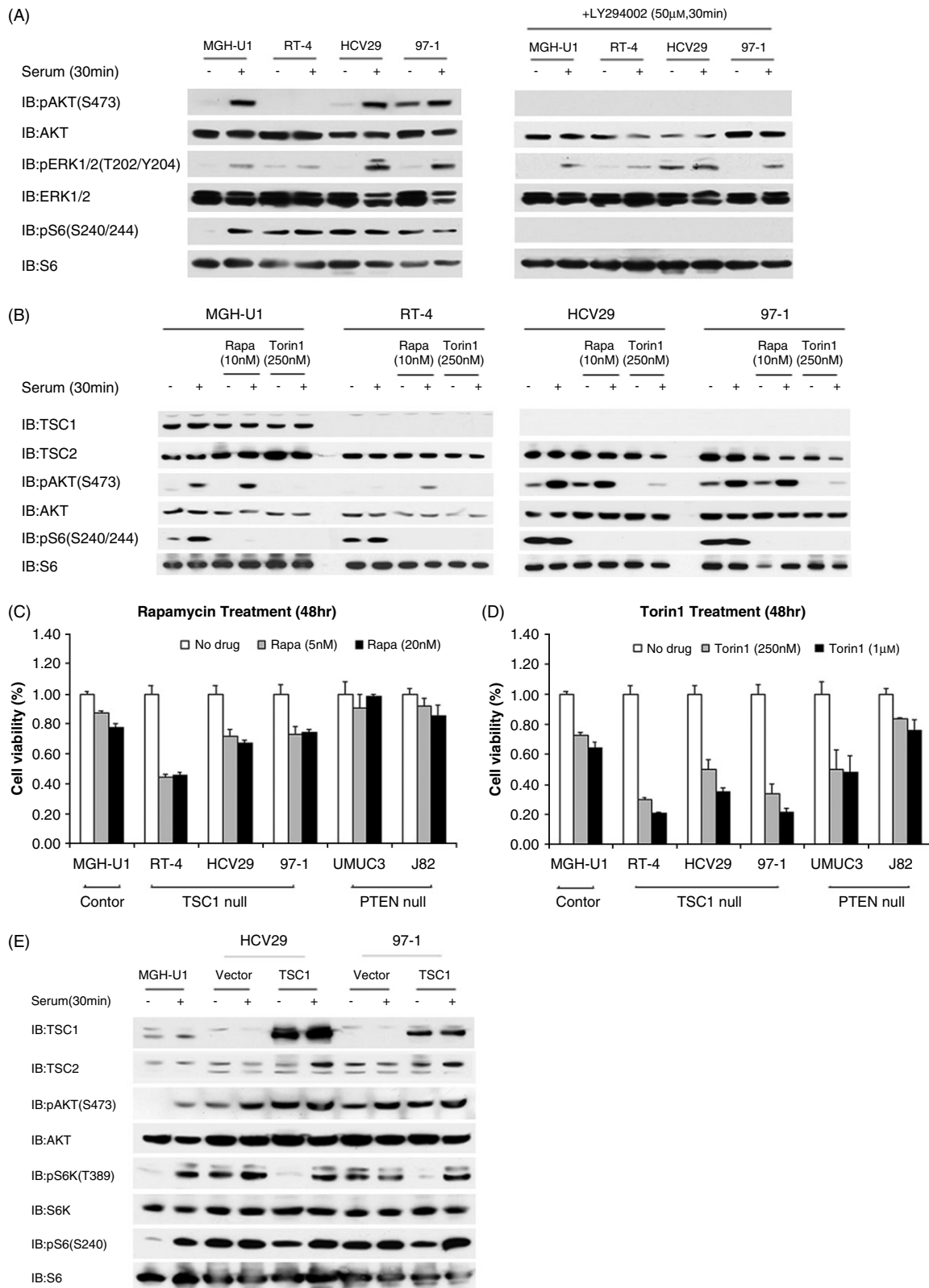


Figure 2. Analysis of AKT activation, drug sensitivity and effects of *TSC1* add-back in *TSC1*-null bladder cancer cell lines. (A) Immunoblots of bladder cancer cell lines after 24 h of serum starvation (–) or 30 min after serum add-back following serum starvation (+), in the absence or presence of 50 μM LY294002 for 30 min. Note suppression of both pAKT(S473) and PS6(S240/244) in response to LY294002. These two blots were prepared at the same time and exposed for exactly the same interval. (B) Immunoblots are shown for bladder cancer cell lines after 24 h of serum starvation (–) or 30 min after serum add-back following serum starvation (+) in the presence of the mTOR inhibitors 10 nM rapamycin or 250 nM Torin1 for 24 h. Note reduction in pAKT(S473) in all lines when treated with Torin1. These two blots were prepared at the same time and exposed for exactly the same interval. (C, D) Cell viability assay for cells treated with mTOR inhibitor rapamycin (C) or Torin1 (D) for 48 h at the indicated doses. Cell number was determined by the MTT assay and normalized to vehicle-treated cells. (E) *TSC1* add-back cells were studied by immunoblot after 24 h of serum starvation (–) or 30 min after serum add-back following serum starvation (+) and show normal regulation of S6K phosphorylation.

component of the mTORC2 complex, was reduced in all three *TSC1*-null lines, in comparison to control (Figure 1A). In addition, IRS1 levels were reduced in all three, as has been reported previously as an effect of phosphorylation of IRS1 by S6K and consistent with chronic mTORC1 activation [20]. Activation of S6K, as assessed by phosphorylation at the T389 site, was increased in these three lines under conditions of serum deprivation and levels of pS6(S240/244) were very high in the absence of serum, also consistent with constitutive mTORC1 activation (Figure 1A).

Among the set of 27 cell lines, we identified two cell lines, UMUC3 and J82, which showed no PTEN expression by immunoblotting, and one cell line, UMUC15, in which LKB1 expression was markedly reduced (see Supplementary material, Table S4). Since FGFR3 mutations are common in bladder cancer, we also examined the mutational hotspots in FGFR3 by sequencing in the 27 cell lines. Eight cell lines had mutations in *FGFR3*. We identified a novel stop mutation (Q256X) and seven previously reported mutations, including six cysteine missense and one K650E mutation. None of the three *TSC1*-null cell lines had an *FGFR3* mutation, although the 639V line with heterozygous missense mutations in *TSC1* had an *FGFR3* R248C mutation.

Differential AKT activation in three *TSC1*-null bladder cancer cell lines

Since HCV29 and 97-1 showed AKT activation, we hypothesized that additional events had occurred in these two cell lines that contributed to that phenomenon, as well as to bladder cancer development, in the patients from whom they were derived. Consequently, we examined this pathway in further detail. First, we observed that treatment of HCV29 and 97-1 cells with the PI3K inhibitor LY294002 completely eliminated pAKT(S473) levels (Figure 2A), independent of serum treatment, suggesting that PI3K activity was required for the activation of AKT. Similarly, treatment of these cells with Torin1, an ATP-competitive inhibitor of mTOR which inhibits both mTORC1 and mTORC2 [21], also eliminated pAKT(S473) levels (Figure 2B). In contrast, mTORC1-specific inhibitor rapamycin either had no effect or caused a minor increase in pAKT(S473) in some conditions (Figure 2B). This confirmed that mTORC2 was functioning as the proximate kinase to phosphorylate AKT at the S473 site [22]. Both Torin1 and rapamycin markedly inhibited mTORC1 activity, as indicated by absence of pS6(S240/244) with those agents (Figure 2B).

We then examined the effects of mTOR inhibitors rapamycin and Torin 1 on the growth of *TSC1*-null bladder cancer cells. RT-4 showed the greatest growth inhibition of all cell lines tested in response to each drug (Figure 2C, D). Torin1 had greater growth inhibitory effects in all three *TSC1*-null cell lines compared to rapamycin. We also generated

TSC1-expressing stable cell lines from HCV29 and 97-1. In comparison to vector-transfected controls, *TSC1* re-expression inhibited mTORC1 activation, as indicated by reduced pS6K(T389) and pS6(S240) under serum-starvation conditions, but had little effect on pAKT(S473) levels (Figure 2E). These results

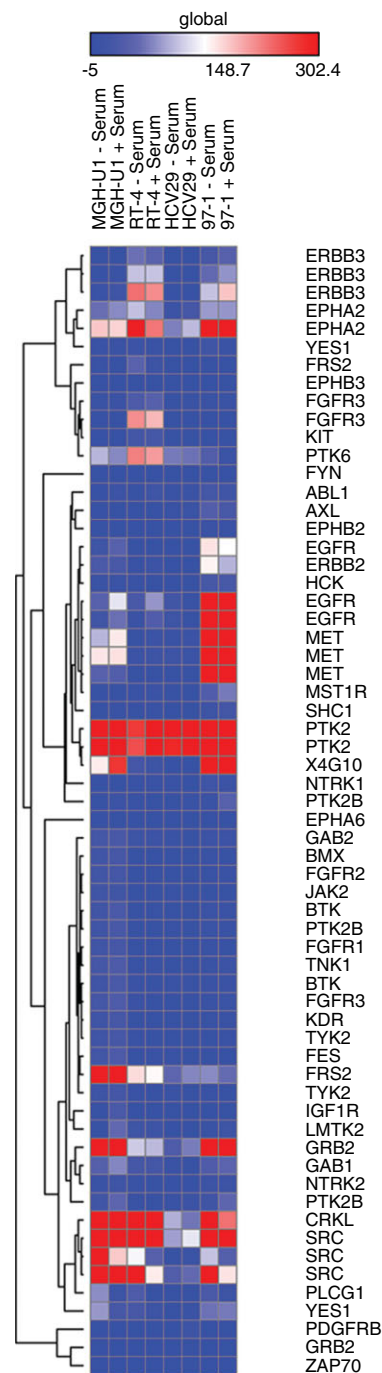


Figure 3. Tyrosine kinase phosphorylation profiling shows EGFR phosphorylation in the bladder cancer cell line 97-1. Human bladder cancer cell lines MGH-U1, RT-4, HCV29 and 97-1 were serum-starved for 24 h (-Serum) or treated with serum for 30 min following serum starvation (+Serum). Cell lysates were analysed by Luminex immunosandwich assays for the phosphorylation of tyrosine kinases. Normalized results are shown, with the colour scale indicating relatively increased (red) or decreased (blue) phospho-protein levels.

provided further evidence to support our hypothesis that other events were influencing AKT activation in the two *TSC1*-null cell lines, HCV29 and 97-1, beyond *TSC1* loss.

Tyrosine kinase profiling indicates that EGFR pathway is activated in the *TSC1*-null bladder cancer cell line 97-1

The finding that activation of AKT was PI3K- and mTORC2- dependent suggested that upstream kinase activation was driving PI3K activation in HCV29 and 97-1 cells. To screen for kinases activating AKT, we performed bead-based profiling of tyrosine kinase phosphorylation [23]. Both EGFR and MET were highly phosphorylated in 97-1 cells, in both serum-deprived and add-back conditions, in contrast to controls (Figure 3; see also Supplementary material, Table S5). To examine the contribution of EGFR activation to both AKT activation and growth, 97-1 cells were treated with two EGFR inhibitors, Lapatinib [24] and Afatinib [25]. Both drugs markedly reduced pAKT(S473) as well as pEGFR(Y1086) levels, independent of serum, and had growth-inhibitory effects (Figure 4A). However, these EGFR inhibitors had little effect on mTORC1 activity, as assessed by persistent high pS6(S240) levels, consistent with the effects of *TSC1* loss (Figure 4A). For this reason, we explored the combination of Lapatinib and Torin1. At low doses, Lapatinib and Afatinib alone each reduced the growth of 97-1 cells. However, the combination of Torin1 or rapamycin with either Lapatinib or Afatinib led to

stronger inhibition of cell growth, and induction of cell death at 1 μ M Lapatinib and at each of 100 nM and 1 μ M Afatinib (Figure 4B-E). We then examined the effects of treatment with these combinations in other bladder cancer cell lines, to examine the specificity of this effect. In contrast to the findings with 97-1, although Lapatinib had growth-suppressing effects on four other bladder cancer cell lines, including two with loss of *TSC1* expression, there was minimal or no synergy when Lapatinib was combined with Torin1 or rapamycin at either low or high dosage (see Supplementary material, Figure S2).

AKT activation in *TSC1*-null bladder cancer cell line HCV29 is BRAF-dependent and ERK-independent

We then sought to identify other gene mutations which might account for the relatively high pAKT(S473) levels seen in the HCV29 and 97-1 cell lines. We assessed the OncoMap panel of 983 mutations in 115 genes [26], including the RAS genes, *PI3KCA* and *AKT*, on those two cell lines, RT-4, and four additional control bladder cancer cell lines (Table 1). HCV29 cells had the *BRAF* missense mutation G469V, while 97-1 had no mutations identified in this assay. *BRAF* G469V has been found in several human cancers, including melanomas [27,28], lung cancer [29] and colorectal cancer [30], and has activating effects on BRAF [31]. To assess the potential effects of the *BRAF* G469V mutation on AKT activation, we treated HCV29 cells with the BRAF kinase inhibitor PLX-4032 (Vemurafenib) [32]. PLX-4032 inhibited AKT activation at

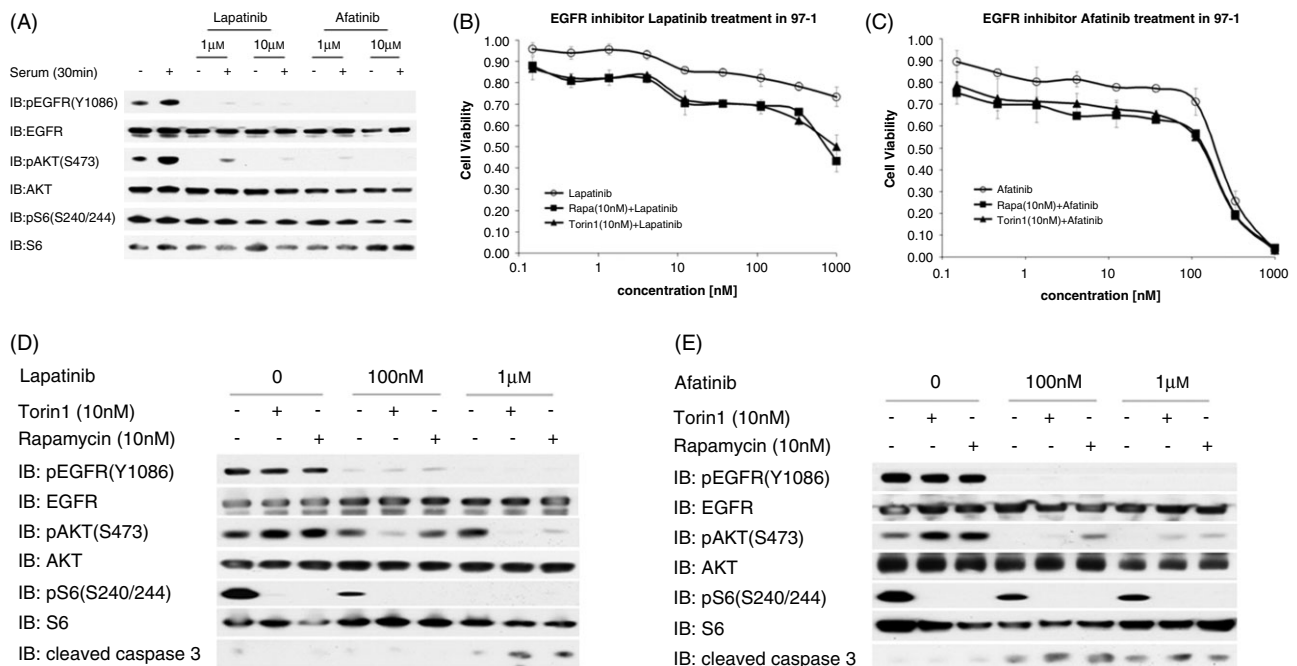


Figure 4. Synergistic effects of EGFR and mTOR inhibition on the *TSC1*-null cell line 97-1. (A) Immunoblotting of 97-1 cells treated with the EGFR inhibitors Lapatinib or Afatinib for 24 h in the presence or absence of serum. (B, C) Cell viability assays (MTT) of 97-1 cells after various treatments: (B) Lapatinib alone or with Torin1 or rapamycin treatment for 48 h; (C) Afatinib alone or with Torin1 or rapamycin treatment for 48 h. (D, E) Immunoblotting of 97-1 cells treated with EGFR inhibitor Lapatinib (D) or Afatinib (E), alone or together with Torin1 (10 nM) or rapamycin (10 nM) in the absence of serum for 24 h.

Table 1. OncoMap gene mutation profiling in bladder cancer cell lines

Cell lines	Sanger sequencing	OncoMap	
	<i>TSC1</i> mutation	Gene mutation	Mutant allele frequency (%)
T-24	-	<i>HRAS</i> G12V	80–90
HT1376	-	-	-
MGH-U1	-	-	-
RT-4	1669 del C	-	-
HCV29	C163T (Q55X)	<i>BRAF</i> G469V	50
97-1	C2074T (R692X)	-	-
639V	T853G (F285V)	<i>CDKN2A</i> R58X	50
	C1849G (H617D)	<i>FGFR3</i> R248C	90
		<i>PTEN</i> R130Q	50
		<i>PTEN</i> R173C	50
		<i>TP53</i> R248Q	100

Seven bladder cancer cell lines were assessed for the OncoMap panel of 983 mutations in 115 genes [26], including *PIK3CA* and *AKT*.

100 nM or higher concentrations (Figure 5A) but had no effect on cell proliferation, similar to a previous report on the effect of this drug in another cell line with *BRAF* G469V mutation [31]. In addition, PLX-4032 combined with either Torin1 or rapamycin had no growth effect on HCV29 cells (Figure 5B). Treatment with the MEK inhibitor U0126 completely eliminated phosphorylation of ERK1/2(T202/Y204) but had no effect on pAKT(S473) levels (Figure 5C), suggesting that ERK and AKT activation were independent events.

Hsp90 inhibitor has synergistic effects with mTOR inhibitor Torin1 or rapamycin to reduce survival of HCV29 cells

To attempt to identify a kinase pathway driving growth of HCV29 cells, we performed a kinase inhibitor screen and included 97–1 cells in this assay. A small-molecule kinase inhibitor library, LINCS, consisting of 197 kinase inhibitors, was used (see Supplementary material, Table S1). Inhibitors were screened both alone and in combination with each of the mTOR inhibitors Torin1 (50 nM) and rapamycin (25 nM), using assessment of cell proliferation with CellTiter-Glo. The initial screen identified five compounds with an $IC_{50} < 660$ nM, for one or both cell lines, alone or in combination with Torin1 or rapamycin (Table 2). We then assayed all five compounds alone and in combination with Torin1 and rapamycin to determine the IC_{50} for each cell line (Table 2). The Hsp90 inhibitor NVP-AUY922 showed a strong synergistic effect with each mTOR inhibitor on HCV29 cells, with a relative reduction in IC_{50} of 316- and 165-fold for Torin1 and rapamycin, respectively, in comparison to NVP-AUY922 alone (Table 2, Figure 6A). In addition, NVP-AUY922 at 100 nM completely eliminated pAKT levels and induced cell death, as indicated by cleaved caspase 3 (Figure 6B). Although NVP-AUY922 inhibited activation of ERK1/2, it had no effect on the stability of BRAF protein, suggesting that *BRAF* mutation was not the main driver of HCV29 cell growth

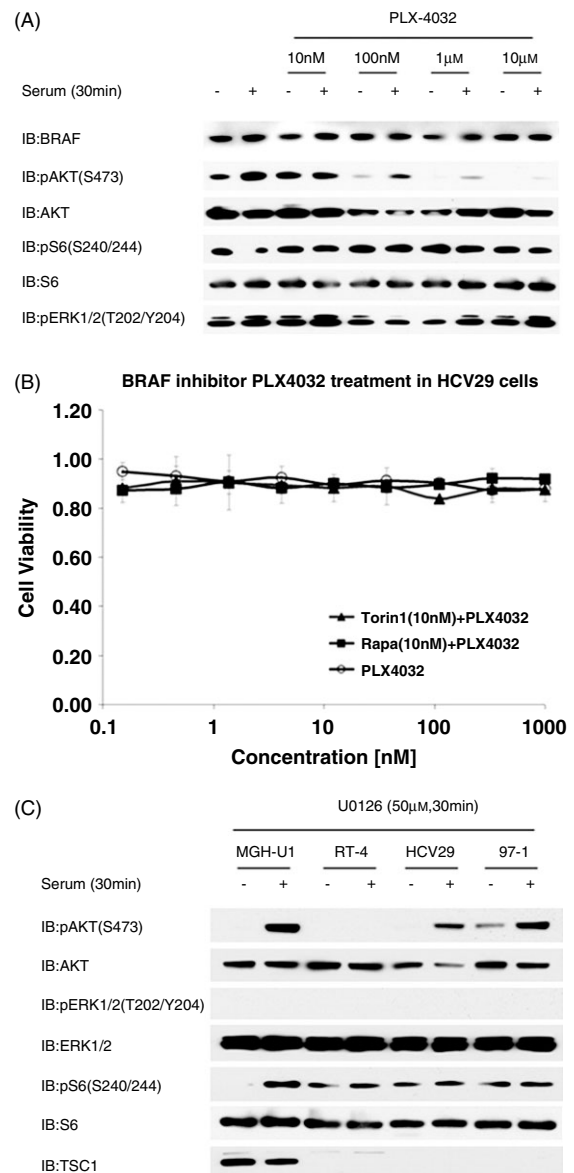


Figure 5. AKT activation in *TSC1*-null line HCV29 is BRAF-dependent and ERK-independent. (A) HCV29 cells were treated with the BRAF inhibitor PLX-4032 for 24 h in the presence or absence of serum and analysed by immunoblotting. Note reduction in pAKT(S473) in response to PLX-4032. (B) Cell viability analysis of HCV29 cells after treatment with PLX-4032 alone or with Torin1 or rapamycin for 48 h. (C) HCV29 cells and controls were treated with the MEK inhibitor U0126 for 30 min in the absence or presence of serum, and analysed by immunoblotting. Immunoblots were done simultaneously with those shown in (A).

(Figure 6B). NVP-AUY922 also demonstrated synergy when applied to 97–1 cells, but to a smaller extent, 3.6- and 29-fold, respectively, for Torin1 and rapamycin (Table 2B). Nonetheless, this combination of an Hsp90 inhibitor and an mTOR inhibitor may have general utility for treatment of *TSC1*-deficient bladder cancer.

Discussion

Bladder cancer is the fourth most common cancer in the USA, with a desperate need for improved

Table 2. Kinase inhibitor IC₅₀ (μM) values for each compound alone or combined with Torin1 or rapamycin

(A) HCV29 cells				
Drug	Target	+DMSO	+Torin1 (10 nM)	+Rapamycin (10 nM)
ZG-10	JNK	3.24	2.05	1.92
YM201636	PI3K	3.78	3.34	2.16
GSK1363089	c-Met	2.28	0.58	0.52
NVP-AUY922	Hsp90	0.83	0.00263	0.00503
MBS-540215	VEGFR	9.47	4.70	4.78
(B) 97-1 cells				
Drug	Target	+DMSO	+Torin1 (3 nM)	+Rapamycin (3 nM)
ZG-10	JNK	1.12	0.86	0.33
YM201636	PI3K	3.49	1.79	0.42
GSK1363089	c-Met	2.02	0.75	0.29
NVP-AUY922	Hsp90	0.54	0.15	0.02
MBS-540215	VEGFR	8.06	5.29	2.21

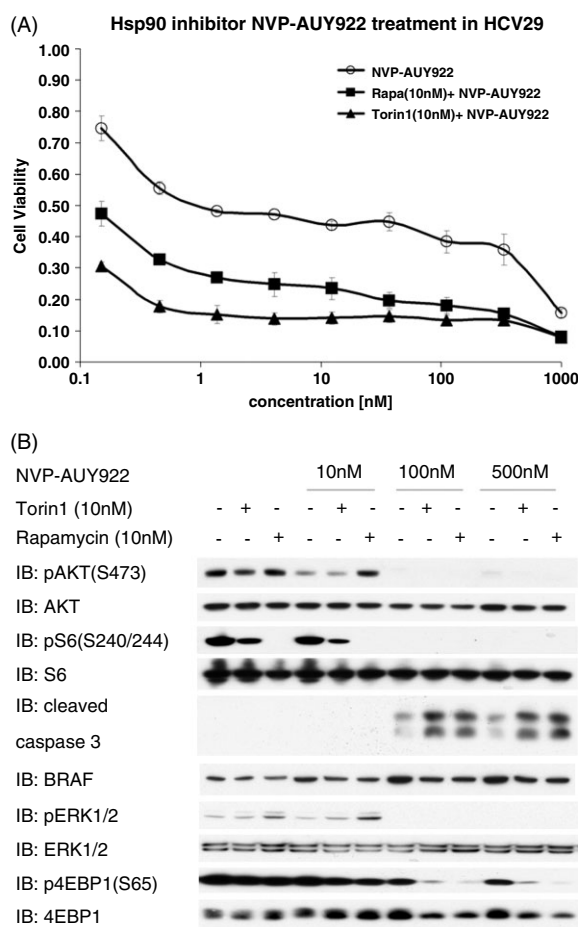


Figure 6. Hsp90 inhibitor has a strong synergistic effect with mTOR inhibitor in HCV29 cells. (A) Cell viability analysis of HCV29 cells after treatment with the Hsp90 inhibitor NVP-AUY922, alone or with Torin1 or rapamycin for 48 h. (B) Immunoblots of HCV29 treated with NVP-AUY922 (10, 100 or 500 nM) in the absence or presence of Torin1 (10 nM) or rapamycin (10 nM) for 24 h.

therapies [1]. Previous reports have indicated that *TSC1* mutations are seen in 10–15% of bladder cancers [7,8,33], similar to the incidence we found here in bladder cancer primary specimens [two (5%) of 41] and bladder cancer cell lines [three (11%) of 27]. *TSC2*-inactivating mutations have also been recently reported in five (3%) of 145 bladder cancer

samples [33]. However, we saw *TSC2* expression in all 27 of our bladder cancer cell lines.

Three bladder cancer cell lines that had homozygous inactivating mutations in *TSC1* and no *TSC1* expression were studied in detail. Strikingly, two of these did not show the classic feedback inhibition of AKT activation that is now well established in MEF and other cell lines lacking *TSC1*–*TSC2* expression [19,20]. Several mechanisms of AKT feedback inhibition have been described in cells lacking the TSC protein complex, including reduction in expression of IRS1 [20] or PDGFR [19,34] or elevated levels of GRB10 [15,16]. Many other phosphorylation targets of S6K have been identified in cells lacking a functional *TSC1*–*TSC2* complex, and these may also contribute to feedback inhibition of this pathway. We confirmed that IRS1 levels were reduced in all three cell lines and established that AKT activation in HCV29 and 97–1 was dependent on mTORC2, consistent with its known function as the kinase which phosphorylates AKT at the S473 site [22].

However, the HCV29 and 97–1 lines had different mechanisms of activation of AKT and growth sensitivities. HCV29 cells had a *BRAF* G469V mutation and AKT activation was very sensitive to treatment with the *BRAF* kinase inhibitor PLX-4032 (Figure 5A). However, PLX-4032 had no effect on HCV29 proliferation as a single agent and did not enhance the growth inhibitory effects of Torin1 or rapamycin (Figure 5B). A kinase inhibitor drug screen identified the Hsp90 inhibitor NVP-AUY922 as having substantial growth inhibitory effects on HCV29. Further, NVP-AUY922 showed strong synergism with mTOR inhibitors, both rapamycin and Torin1, in reducing the growth and inducing cell death of HCV29 cells (Figure 6B). The combination of an Hsp90 and an mTOR inhibitor has recently been reported to be highly effective in both Nf1-deficient and Kras-driven cancers, through enhancement of ER stress, ROS generation and oxidative stress [35]. Since loss of *TSC1*–*TSC2* is known to lead to ER stress [36,37], it is quite possible that the same mechanism applies in this instance. It is uncertain whether there is a single critical client protein for Hsp90 inhibition in HCV29 cells, or

whether this growth inhibition is a synergistic effect dependent on reduced expression of multiple client proteins.

97–1 cells also showed EGFR and MET phosphorylation and activation in a proteome kinase assay and were sensitive to the EGFR inhibitors, Lapatinib and Afatinib, as assessed by effects on both pAKT(S473) and pEGFR(Y1086) levels (Figure 4A). These drugs did not affect mTORC1 activity, but each showed synergistic effects in growth inhibition in combination with Torin1 and rapamycin (Figure 4B–E). Control experiments showed that these effects were unique to 97–1, suggesting a dependency upon both EGFR and mTORC1 activation for this drug sensitivity. 97–1 cells were also highly sensitive to combined Hsp90-mTOR inhibition.

In aggregate, these results point to significant heterogeneity among the three bladder cancer cell lines we studied that had complete loss of *TSC1*, suggesting that a ‘personalized’ approach to therapy for the corresponding cancers would be most effective. Recently a dramatic and sustained clinical response to everolimus, a compound closely related to rapamycin, has been reported in a patient with metastatic bladder cancer bearing a *TSC1*-inactivating mutation [10]. However, four other patients in that study with inactivating mutations in *TSC1* showed short-lived minimal responses to everolimus. Hence, these clinical findings are similar to those presented here, indicating the heterogeneity of growth mechanisms operative in bladder cancers with *TSC1* mutation and loss and the need for individualized therapy for these cancers. Hsp90 inhibition in combination with mTORC1 inhibition has promise for this class of bladder cancer.

Acknowledgements

We thank Dr Pasi A Janne and Krishna M Vasudevan (Dana Farber Cancer Institute, MA, USA) for kindly providing inhibitors used in this study; Margaret A Knowles (St James’s University Hospital, UK) for kindly providing the HCV29 and 97–1 bladder cancer cell lines; and Laura McConaill for assistance with the Oncomap screen. This study was supported by the National Institutes of Health (Grant No. 1P01CA120964).

Author contributions

YG planned and performed experiments, performed data analysis and wrote the manuscript; YC, JZ and JD performed experiments, analysed data, contributed manuscript sections and reviewed the manuscript; NG proposed experiments, oversaw performance and data collection of experiments and reviewed the manuscript; and CW and DJK planned and guided experiments, reviewed all data and wrote the manuscript.

References

1. Siegel R, Naishadham D, Jemal A. Cancer statistics, 2012. *CA Cancer J Clin* 2012; **62**: 10–29.
2. Epstein JI, Amin MB, Reuter VR, et al. The World Health Organization/International Society of Urological Pathology consensus classification of urothelial (transitional cell) neoplasms of the urinary bladder. Bladder Consensus Conference Committee. *Am J Surg Pathol* 1998; **22**: 1435–1448.
3. Wu X, Ros MM, Gu J, et al. Epidemiology and genetic susceptibility to bladder cancer. *BJU Int* 2008; **102**: 1207–1215.
4. Habuchi T, Devlin J, Elder PA, et al. Detailed deletion mapping of chromosome 9q in bladder cancer: evidence for two tumour suppressor loci. *Oncogene* 1995; **11**: 1671–1674.
5. Chang LL, Yeh WT, Yang SY, et al. Genetic alterations of *p16INK4a* and *p14ARF* genes in human bladder cancer. *J Urol* 2003; **170**: 595–600.
6. Knowles MA, Habuchi T, Kennedy W, et al. Mutation spectrum of the 9q34 tuberous sclerosis gene *TSC1* in transitional cell carcinoma of the bladder. *Cancer Res* 2003; **63**: 7652–7656.
7. Knowles MA, Platt FM, Ross RL, et al. Phosphatidylinositol 3-kinase (PI3K) pathway activation in bladder cancer. *Cancer Metast Rev* 2009; **28**: 305–316.
8. Pymar LS, Platt FM, Askham JM, et al. Bladder tumour-derived somatic *TSC1* missense mutations cause loss of function via distinct mechanisms. *Hum Mol Genet* 2008; **17**: 2006–2017.
9. Goebell PJ, Knowles MA. Bladder cancer or bladder cancers? Genetically distinct malignant conditions of the urothelium. *Urol Oncol* 2010; **28**: 409–428.
10. Iyer G, Hanrahan AJ, Milowsky MI, et al. Genome sequencing identifies a basis for everolimus sensitivity. *Science* 2012; **338**: 221.
11. Kwiatkowski DJ, Thiele E, Whittemore VH. *Tuberous Sclerosis Complex*. Wiley-VCH: Weinheim, Germany, 2010: 3–7.
12. Tee AR, Fingar DC, Manning BD, et al. Tuberous sclerosis complex-1 and -2 gene products function together to inhibit mammalian target of rapamycin (mTOR)-mediated downstream signaling. *Proc Natl Acad Sci USA* 2002; **99**: 13571–13576.
13. Yecies JL, Manning BD. Transcriptional control of cellular metabolism by mTOR signaling. *Cancer Res* 2011; **71**: 2815–2820.
14. Zoncu R, Efeyan A, Sabatini DM. mTOR: from growth signal integration to cancer, diabetes and ageing. *Nat Rev Mol Cell Biol* 2011; **12**: 21–35.
15. Hsu PP, Kang SA, Rameseder J, et al. The mTOR-regulated phosphoproteome reveals a mechanism of mTORC1-mediated inhibition of growth factor signaling. *Science* 2011; **332**: 1317–1322.
16. Yu Y, Yoon SO, Poulgiannis G, et al. Phosphoproteomic analysis identifies Grb10 as an mTORC1 substrate that negatively regulates insulin signaling. *Science* 2011; **332**: 1322–1326.
17. van Slegtenhorst M, de Hoogt R, Hermans C, et al. Identification of the tuberous sclerosis gene *TSC1* on chromosome 9q34. *Science* 1997; **277**: 805–808.
18. Chong-Kopera H, Inoki K, Li Y, et al. *TSC1* stabilizes *TSC2* by inhibiting the interaction between *TSC2* and the *HERC1* ubiquitin ligase. *J Biol Chem* 2006; **281**: 8313–8316.
19. Zhang H, Cicchetti G, Onda H, et al. Loss of *Tsc1/Tsc2* activates mTOR and disrupts PI3K–Akt signaling through downregulation of PDGFR. *J Clin Invest* 2003; **112**: 1223–1233.
20. Harrington LS, Findlay GM, Gray A, et al. The *TSC1–2* tumor suppressor controls insulin–PI3K signaling via regulation of IRS proteins. *J Cell Biol* 2004; **166**: 213–223.
21. Thoreen CC, Kang SA, Chang JW, et al. An ATP-competitive mammalian target of rapamycin inhibitor reveals rapamycin-resistant functions of mTORC1. *J Biol Chem* 2009; **284**: 8023–8032.
22. Sarbassov DD, Guertin DA, Ali SM, et al. Phosphorylation and regulation of Akt/PKB by the rictor–mTOR complex. *Science* 2005; **307**: 1098–1101.

23. Du J, Bernasconi P, Clauser KR, *et al.* Bead-based profiling of tyrosine kinase phosphorylation identifies SRC as a potential target for glioblastoma therapy. *Nat Biotechnol* 2009; **27**: 77–83.
24. Xia W, Mullin RJ, Keith BR, *et al.* Anti-tumor activity of GW572016: a dual tyrosine kinase inhibitor blocks EGF activation of EGFR/erbB2 and downstream Erk1/2 and AKT pathways. *Oncogene* 2002; **21**: 6255–6263.
25. Eskens FA, Mom CH, Planting AS, *et al.* A phase I dose escalation study of BIBW 2992, an irreversible dual inhibitor of epidermal growth factor receptor 1 (EGFR) and 2 (HER2) tyrosine kinase in a 2-week on, 2-week off schedule in patients with advanced solid tumours. *Br J Cancer* 2008; **98**: 80–85.
26. MacConaill LE, Campbell CD, Kehoe SM, *et al.* Profiling critical cancer gene mutations in clinical tumor samples. *PLoS One* 2009; **4**: e7887.
27. Willmore-Payne C, Holden JA, Tripp S, *et al.* Human malignant melanoma: detection of *BRAF*- and *c-kit*-activating mutations by high-resolution amplicon melting analysis. *Hum Pathol* 2005; **36**: 486–493.
28. Ugurel S, Thirumaran RK, Bloethner S, *et al.* *B-RAF* and *N-RAS* mutations are preserved during short time *in vitro* propagation and differentially impact prognosis. *PLoS One* 2007; **2**: e236.
29. Ding L, Getz G, Wheeler DA, *et al.* Somatic mutations affect key pathways in lung adenocarcinoma. *Nature* 2008; **455**: 1069–1075.
30. Ikehara N, Semba S, Sakashita M, *et al.* *BRAF* mutation associated with dysregulation of apoptosis in human colorectal neoplasms. *Int J Cancer* 2005; **115**: 943–950.
31. Yang H, Higgins B, Kolinsky K, *et al.* RG7204 (PLX4032), a selective *BRAF*V600E inhibitor, displays potent antitumor activity in preclinical melanoma models. *Cancer Res* 2010; **70**: 5518–5527.
32. Bollag G, Hirth P, Tsai J, *et al.* Clinical efficacy of a *RAF* inhibitor needs broad target blockade in *BRAF*-mutant melanoma. *Nature* 2010; **467**: 596–599.
33. Sjodahl G, Lauss M, Gudjonsson S, *et al.* A systematic study of gene mutations in urothelial carcinoma; inactivating mutations in *TSC2* and *PIK3R1*. *PLoS One* 2011; **6**: e18583.
34. Zhang H, Bajraszewski N, Wu E, *et al.* PDGFRs are critical for PI3K/Akt activation and negatively regulated by mTOR. *J Clin Invest* 2007; **117**: 730–738.
35. De Raedt T, Walton Z, Yecies JL, *et al.* Exploiting cancer cell vulnerabilities to develop a combination therapy for *ras*-driven tumors. *Cancer Cell* 2011; **20**: 400–413.
36. Ozcan U, Ozcan L, Yilmaz E, *et al.* Loss of the tuberous sclerosis complex tumor suppressors triggers the unfolded protein response to regulate insulin signaling and apoptosis. *Mol Cell* 2008; **29**: 541–551.
37. Di Nardo A, Kramvis I, Cho N, *et al.* Tuberous sclerosis complex activity is required to control neuronal stress responses in an mTOR-dependent manner. *J Neurosci* 2009; **29**: 5926–5937.
38. Wang Y, Carlton VE, Karlin-Neumann G, *et al.* High quality copy number and genotype data from FFPE samples using molecular inversion probe (MIP) microarrays. *BMC Med Genomics* 2009; **2**: 8.
39. Yvonne C, Chin-Lee W, Jonathan R, *et al.* Identification of nine genomic regions of amplification in urothelial carcinoma, correlation with stage, and potential prognostic and therapeutic value. *PLOS ONE* 2013 [in press].

SUPPORTING INFORMATION ON THE INTERNET

The following supplementary material may be found in the online version of this article:

Figure S1. Sanger sequencing of *TSC1* in human bladder cancer samples and cell lines

Figure S2. EGFR and mTOR inhibitors show no synergy in several bladder cancer cell lines

Table S1. FGFR Sanger sequencing primers

Table S2. Kinase inhibitor focused library (LINCS)

Table S3. *TSC1* and *TSC2* loss and mutation in human bladder cancer samples

Table S4. Immunoblot and mutation analysis of bladder cancer cell lines

Table S5. Kinome tyrosine kinase activity profiling results